NANO: Brief Reports and Reviews
Vol. 2, No. 1 (2007) 41–49

World Scientific
www.worldscientific.com

DYNAMIC RESPONSE OF CARBON NANOTUBES DISPERSED IN NEMATIC LIQUID CRYSTAL

SANG YOUN JEON*, KYUNG AH PARK†, IN-SU BAIK*,
SEOK JIN JEONG*, SEOK HO JEONG†, KAY HYEOK AN‡,
SEUNG HEE LEE*,§ and YOUNG HEE LEE†,¶

*School of Advanced Materials Engineering
Chonbuk National University
Chonju, Chonbuk 560-756, Korea

†Institute of Basic Science
Center for Nanotubes and Nanostructured Composites
Sungkyunkwan Advanced Institute of Nanotechnology
Sungkyunkwan University, Suwon 440-746, Korea

‡Jeonju Machinery Research Center
Palbok-dong, 750-1, Jeonju 561-844, Korea
§lsh1@chonbuk.ac.kr
¶leeyoung@skku.edu

Received 11 December 2006

The alignment and dynamic response of carbon nanotubes (CNTs) in nematic liquid crystal (NLC) medium induced by strong electric field have been observed through polarizing optical microscope. Density-functional calculations suggest that LC molecule anchors helically to the CNT wall to enhance π-stacking with a binding energy of nearly $-2.0\,\text{eV}$ due to a considerable amount of charge transfer from LC molecule to CNT, resulting in the formation of excess charges and permanent dipole moment in CNTs. Under strong electric field, the motion of CNTs distorted the director of adjacent LC molecules. Our detailed analysis of dynamics revealed that the four-lobe textures in vertical cell and two vertical stripes in in-plane switching cell were strongly correlated, i.e., the side view of textures by the vertical motion of CNTs in vertical cell was similar to the textures in in-plane switching cell. Interestingly, the magnitude of textures in microscope was strongly dependent on the size of CNTs and the applied field strength. The statistical size distribution of textures similar to that of CNTs provided information for the degree of dispersion of CNTs.

Keywords: Carbon nanotube (CNT); liquid crystal (LC); dynamic response; density functional theory (DFT).

1. Introduction

One-dimensional carbon nanotubes (CNTs) have unique atomic and electronic structures. One of the fascinating research areas is the CNT composite where the performance of host materials can be significantly improved by an addition of a small amount of CNTs. The dispersion and alignment of CNTs and nanowires in various composites are an important issue in improving mechanical, electrical, thermal, and optical properties of host materials such as polymers and liquid crystals (LCs).[1–6] In particular, CNTs prefer to aggregate into bundles

due to their primary van der Waals interactions between the micrometer-long CNTs. The superb physical and chemical characteristics of CNTs and device performance are often obscured by such an agglomeration. Surfactants, polymers, and DNA have been introduced to enhance the dispersion of CNTs.[7–10] Yet, these additional dispersants remained in the sample after treatment, introducing an additional difficulty.

Nematic liquid crystal (NLC) studied in this paper is composed of rod-like molecules with an aspect ratio of about 3 to 5 depending on the structure in which its orientational ordering appears when phase transition from isotropic to nematic phase occurs with decreasing temperature. NLC is optically uniaxial and plays a central role in liquid crystal display industry. The alignment of the LC molecules can be controlled by the surface treatment of the substrate and the orientation of LCs can be controlled by an external field that induces Freedericksz transition. Recently, a local orientational order of CNTs has been induced by an assistance of LC director or by pressing CNT-dispersed LC gels.[11,12] Since the length of CNTs is usually on the order of μm and that of LC molecule is on the order of a few nm, it is intriguing to see how such a macroscopic CNT could be aligned in an assemblage of microscopic LC molecules. Although such a preferential alignment is expected to rely on the interactions between CNT and LC molecules, the nature of their mutual interactions has not been clarified yet. In addition, controlling the alignment of CNTs in host materials is challenging and often of technological importance.

It has been known that CNTs altered the device performance of the LC display cells. A minute addition of CNTs in LC medium increased the conductivity of the medium significantly above the threshold voltage to reveal the switching effect.[13] In spite of the preferential alignment of CNTs in LC medium, those CNTs were often visible through optical microscope in a form of bundles and clusters. For a complete alignment of CNTs in LC device such as twisted nematic cell, the CNT effects on electro-optic characteristics were studied. It has been argued that the residual DC, which is related to an image sticking problem in LC displays, was greatly reduced due to the ion trapping by CNTs.[14–16] Another intriguing issue is a transient behavior of the CNT in LC medium under electric field. Since the CNT orientation is strongly affected by the external field, the presence of CNTs in LC medium may invoke the distortion of LC director. This distortion may not be visible through optical microscope due to its small size but could be visible via the phase retardation by the adjacent LC molecules to CNTs through optical polarizing microscope. This provides another means of observing the degree of dispersion of CNTs in the host LC medium, which is not usually available from other materials.

Our aim here is two-fold: (i) to understand the interaction between nanotube and LC molecule and (ii) to understand various pattern dynamics of CNTs generated in LC cell. CNTs were well dispersed in super-fluorinated LC medium in dichloroethane (DCE) solvent with a mild sonication. This was strongly related to the interaction between the CNT and LC molecule. From density functional calculations, we found that the interaction energy between CNT wall and fluorinated LC molecule was close to -2 eV, and furthermore a significant amount of charge transfer occurred from LC molecule to CNT. We observed various pattern formations of four-lobed and stripe patterns in LC/CNT composite cell above threshold AC fields. Slow dynamics clearly revealed that the patterns were generated by the motion of CNTs with an excess charge and permanent dipole moment in LC medium that generated various pattern dynamics. The analysis of the observed patterns also provided useful information for the degree of dispersion of CNTs in LC medium. Our approach helps to understand interactions between the anisotropic solids and the LC solvent, and opens a new possibility to use them as a means of observing their dynamic response in LC medium.

2. Experimental and Theoretical Methods

Thin multi-walled carbon nanotubes (t-MWCNTs) were synthesized by chemical vapor deposition (CVD) method using FeMoMgO catalysts prepared by combustion method. The outer diameter of the pristine t-MWCNTs ranged from 3 to 6 nm with typical lengths of 0.1–1.5 μm. The outmost nanotubes were presumably metallic, because of its large diameters of 3–6 nm. The inner diameter of the pristine t-MWCNTs ranged from 0.7 to 2.6 nm, which was confirmed by the radial breathing mode of Raman spectra. The integration intensity of the

D-band in Raman spectra near 1320 cm^{-1} was much smaller than that of the CVD-grown multiwalled carbon nanotubes, suggesting high crystallinity of our sample. The remaining metal content with MgO supporters was 3.5 wt%. This has been described in details elsewhere.[17] Since the volume ratio of metal content to the t-MWCNTs was much smaller than that of mass ratio, this as-grown sample was directly used without further purification in this study. 10 mg t-MWCNT powders were dispersed in DCE of 100 ml by sonication for 24 h. The supernatant was decanted after centrifugating at 15 000 rpm for 30 min. The most common CNT lengths in the supernatant after sonication were 250 nm, which was observed from the tapping mode of atomic force microscopy (AFM: Seiko SPA-400).

The supernatant with a CNT concentration of 20.6 g/ml was poured in a nematic LC solution (super-fluorinated LC mixtures used generally in thin-film-transistor-LC displays from Merck-Japan with physical properties, dielectric anisotropy $\Delta\varepsilon = 7.4$, birefringence $\Delta n = 0.88$ at $\lambda = 589$ nm, clearing temperature 87°C with a nematic phase down to −40°C). After sonication of this mixture for 10 min, the DCE solvent was then removed using a solvent evaporator. The t-MWCNT/LC solutions with different CNT concentrations of 0.0001, 0.0005, 0.001, 0.01 wt% were further sonicated for 10 min. The HiPco SWCNTs (Carbon Nanotechnology Inc.) were also used for comparison using similar procedure. Since the carbon nanotubes are conductive, the conductivity of the LC cell can be increased slightly especially at high CNT concentrations. The effect of operation voltage and charge trapping by CNT doping has been described elsewhere.[15] The direct dissolution of CNTs in nematic LC solution resulted in an agglomeration of CNTs as observed previously.[18] Since the DCE is known as the best solvent to nanodisperse SWCNTs and can be easily evaporated, the current approach allows CNTs to disperse ideally in LC medium.

Two different cells with homogeneous and homeotropic alignment driven by vertical electric field were fabricated using alignment layers of AL16139 and AL00010 (Japan Synthetic Rubber Co.), respectively. The homogeneous and homeotropic cells with an area of 3×3 cm^2 and a cell gap of 60 μm were made using an indium-tin-oxide (ITO)-coated glass. Another cell with homogeneous alignment but driven by in-plane electric field was fabricated, in which the electrodes exist only on one substrate with electrode width of 10 μm and distance of 30 μm between them. The LC director was aligned parallel to the in-plane field, and the cell gap was 9 μm. The CNT/LC mixture was then filled into the cell by a capillary force at room temperature. The electro-optical textures of the test cell were observed by the optical polarizing microscope (Nikon DXM1200) by applying either AC or DC voltage.

Our total energy calculations and corresponding structure optimizations of the most stable geometries are based on the density functional formalism within the local density approximation (LDA) and the generalized gradient approximation (GGA), as implemented in DMol^3 code.[19,a] The exchange-correlation energy in LDA is parameterized by the Perdew and Wang's scheme,[20] and Becke's corrected exchange functional[21] is adopted in GGA. All-electron Kohn–Sham wave functions are expanded in a local atomic orbital basis set with each basis function defined numerically on an atomic-centered spherical polar mesh. We used a double numeric polarized basis set, which is the most complete set available in DMol^3 code. In this basis set, the $2s$ and $2p$ carbon, fluorine, oxygen orbitals are represented by two wave functions each, and a $3d$ ($2p$) type wave functions on each carbon, fluorine, and oxygen (hydrogen) atoms are used to describe the polarization. No frozen core approximation is used throughout calculations. For accurate binding energy calculations, GGA calculations are performed after geometrical optimization by LDA. The forces on each atom to be converged during each relaxation are less than 10^{-3} atomic units.

The LC molecule is composed of a head part with polarity, a rigid part with hexagonal rings, and a tail part with alkyl groups. The choice of these groups plays an important role in determining interaction with CNT walls, when CNTs are added in LC medium. A vast molecular library can be formed by different functional groups at the head part and a number of rings that seemingly induce anchoring on the CNT walls via π-stacking interaction. Commercially available thin-film transistor-LC display utilizes the

[a]DMol^3 is a registered software product of Accelrys Inc.

mixture of super-fluorinated LC molecules, which have a good reliability in thermal and ultraviolet stress and are known to be advantageous over the conventional cyan-functionalized ones.[22] Therefore, we chose a typical super-fluorinated LC molecule, trifluorophenyl-2 (TFP2) as a model of calculation, which was introduced in experiments. This molecule is composed of hexagonal head part with three fluorine atoms, two cyclohexane rings, and alkyl chain tail part. We chose (5, 5) armchair CNT with CNT length of 14 layers along the tube axis. We studied three cases of open nanotube, hydrogen-, and oxygen-terminated nanotubes to emulate the functionalized CNTs which were the usual situation after acid treatment.

3. Results and Discussion

The CNT/LC orientation in homogeneously and homeotropically aligned cells at different t-MWCNT concentrations under no bias voltage is presented in Fig. 1. In a homogeneously aligned cell, the LC director was aligned parallel to the surface and its optical axis was coincident with one of the crossed polarizer axes so that the cell manifested a nematic dark state, as shown in Fig. 1(a). The LC orientation was not perturbed by an addition of t-MWCNT with the concentration of 0.001 wt%, and the cell retained a complete dark state. This implied that the presence of rod-like CNTs did not disturb the LC director in the cell at the microscopic scale. This is in good agreement with the previous observations that CNTs were pushed to align themselves along the LC director in the LC medium.[11] It is remarkable that the long CNTs with a length of about 250 nm were restricted to orient by an assembly of small LC molecules with a length of a few nm. On the other hand, at high t-MWCNT concentration of 0.01 wt%, the LC orientation was disturbed around the CNT clusters so that the leakage due to deviation of the LC optic axis from the transmission axes of the crossed polarizers occurred and the closed loop patterns with light transmission randomly spread in the cell, as shown in Fig. 1(b). Similar phenomenon was observed in the homeotropically aligned cell, as shown in Figs. 1(c) and 1(d). The LC molecules were initially aligned perpendicular to

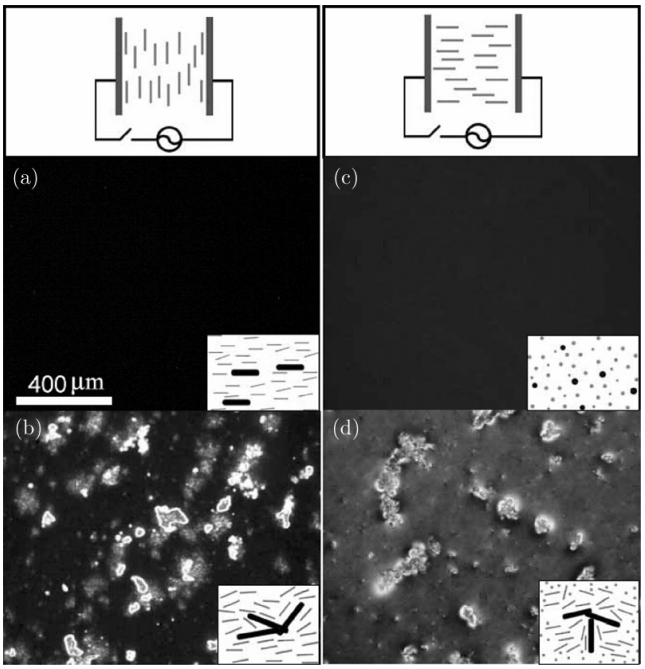

Fig. 1. Optical polarizing microscopic photographs of [(a) and (b)] homogeneous and [(c) and (d)] homeotropic cells with different CNT concentrations of [(a) and (c)] 0.001 wt%, and [(b) and (d)] 0.01 wt% without bias voltage. The inset indicates the top view of the corresponding molecular orientations of CNT (black rod) and LC molecules (grey color). The top panel indicates the side view of the corresponding cell schematics.

the surface of the homeotropic cell (confirmed by a conoscopic study). Under the crossed polarizers, the cell appeared to be dark. Since the NLC used has a positive dielectric anisotropy, the LC directors will be aligned more strongly under the vertical electric field, thus completing the darkness of the cell. No light leakage was observed with an addition of CNTs (Fig. 1(c)). This clear dark phase simply indicates that the axis of rod-like CNTs is aligned parallel to the LC directors.[b] The persistent CNT alignment through the LC medium would only be possible when LC molecules are strongly anchored on CNT walls such that CNTs are forced to be aligned with LC directors.

In order to understand seemingly strong anchoring of LC molecules on the CNT wall, we performed density functional calculations. We first tried to optimize bare LC molecules. Among several types of TPF2 conformation, we found chair–chair conformation (Fig. 2(a)) to be the most

[b]The cell gap in this case was 60 μm, much longer than the CNT lengths of 250 nm. No significant increment of conductivity was observed in this case, unlike the previous studies (see Ref. 11). It seemed that the percolation limit was not reached due to the insufficient scattering of CNTs at this concentration.

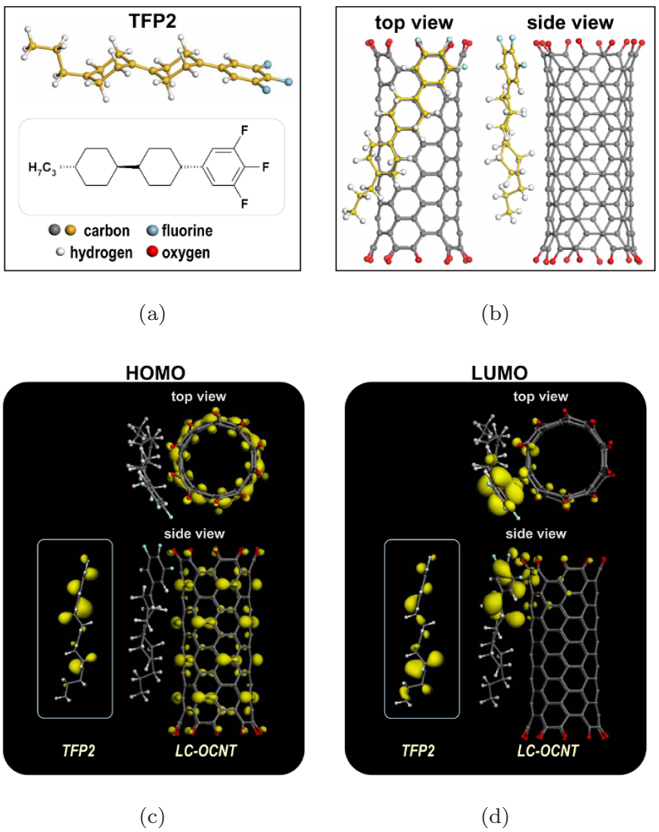

Fig. 2. (a) Ball and stick structure and carbon skeleton diagram of trifluorophenyl2 (TFP2) LC molecule. (b) Top and side views of LC molecule anchored on the CNT sidewall. The dangling bonds in CNT edge were functionalized by oxygen. (c) HOMO and (d) LUMO states of LC and oxygen-terminated CNT. The related HOMO and LUMO of the isolated LC molecule are also presented in the box.

stable geometry.[c] The binding energy between antisymmetric LC molecules was −0.43 eV from LDA calculation, which correlated to the isotropic/nematic phase transition temperature near 80°C.

The binding energy was stronger in oxygen-functionalized CNT, where the amount of charge transfer was 0.73 e, the largest among all species, independent of the calculational methods. This binding energy between LC molecule and the oxygen-functionalized CNT wall was −1.8 eV from LDA calculations, much stronger than LC–LC interaction energy of −0.43 eV. The binding was promoted by (i) increasing contact area and thus hexagon–hexagon π-stacking interaction at the head and rigid parts, resulting in a helical wrapping (Fig. 2(b)) and (ii) the Mulliken charge transfer from LC to CNTs, resulting in electrostatic interaction. This was confirmed by the interaction range of 2.21 Å between hydrogen atoms in LC and carbon atoms on the CNT wall, shorter than the typical van der Waals interaction range. One clearly see that the electron charges were transferred from the highest occupied molecular orbital (HOMO) localized at the head part of LC molecule to that of the CNT. On the other hand, the lowest unoccupied molecular orbital (LUMO) at the head part of LC molecule was increased. Thus the head part of the LC molecule plays an important role in determining the binding energy. The details will be described elsewhere.[23] This strong binding energy is responsible for a preferential alignment of CNTs in LC cell under no bias voltage and will promote the dispersion of CNTs in the host LC medium.

So far we described CNTs with strongly anchored LC molecules in the surrounding that were well aligned along the initial LC director on the surface in the absence of field. This alignment was not altered, i.e., no change in the dark phase until high AC voltage up to 50 V for the homeotropic cell was applied. Figure 3 presents the patterns generated above threshold sine wave voltage at 60 Hz with the corresponding schematics of cells. At high electric field, some spots and/or regular patterns started to appear.[d] For instance, in the homeotropic cell, where the LC directors were aligned vertically from the substrate, four-lobe patterns were clearly observed through polarizing optical microscope, as seen in Fig. 3(a). The corresponding patterns through optical microscope were also shown in the bottom panel. These patterns were never visible without CNTs. Therefore, the patterns resulted from CNTs, not from LC molecules. Yet, these pattern shapes of CNTs are similar to those of LC molecules due to their rod-like nature.[24] The four-lobe patterns under polarizing optical microscope are attributed to the phase retardation of the LC medium that leads to the light leakage, generated by the perturbed LC directors due to the translational motion of CNTs.[e]

[c]Additional information is available via http://nanotube.skku.ac.kr/support.html.
[d]Additional information is available via http://nanotube.skku.ac.kr/support.html.
[e]The transmittance is defined by $\sin2(2\psi(V))\sin2(\pi d\Delta n_{\text{eff}}/\lambda)$, where ψ is a voltage-dependent angle between the LC director and crossed polarizer axes, and $d\Delta n_{\text{eff}}$ is also a voltage-dependent effective cell retardation value where d and Δn_{eff} are the cell gap and the effective refractive index, respectively. The motion of CNTs gives rise to the change in effective cell retardation value and thus the transmittance is to be altered.

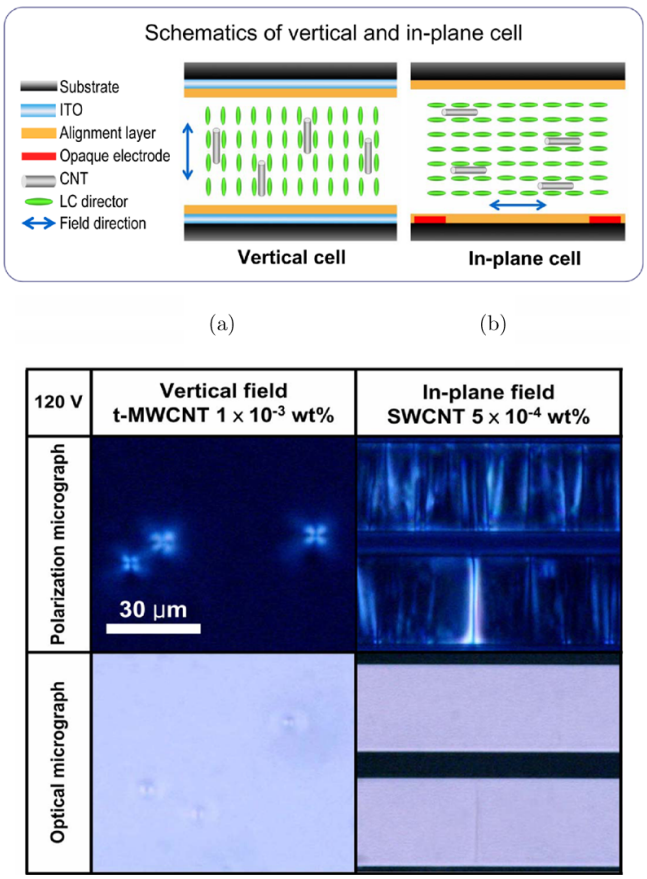

Fig. 3. Optical micrographs with polarizers (upper panel) and without polarizers (lower panel) which were doped by (a) t-MWCNTs of 0.001 wt% and (b) SWCNTs of 0.0005 wt% in the in-plane cell. All images were fixed at the same magnification. The arrows in (b) indicated the radius of the spot area.

These patterns evolved over time. When the field was terminated, the dynamic response of CNTs ceased. The long axis of CNTs was then pushed back to align to LC directors. The cell texture fully recovered to the original dark phase with time. This confirms again that the dynamic response originated from the CNTs, not from the LC directors.

The dynamic response of CNTs can be also monitored through the homogeneous cell driven by in-plane field, where CNTs are aligned parallel to the in-plane field direction between two in-plane electrodes (Fig. 3(b)). Under DC or AC field, the LC molecule, which does not possess an excess charge or a permanent dipole moment, will be aligned along the field direction due to induced dipole moment but will have neither translational nor time-dependent orientational motion. On the other hand, if CNTs possess an excess charge and a permanent dipole moment, under the external field, they will have translational and time-dependent orientational motion that induces distortion of LC directors and as a consequence the light leakage. A transient motion between electrodes was observed above critical DC field, which exhibits a direct evidence of CNTs possessing an excess charge. On the other hand, under AC field above 60 V, the vertical stripes moved back and forth between two electrodes, while maintaining translational motion along electrodes. In this case, the dipole energy of CNTs is huge due to its long length such that they are forced to have an orientational motion along the field direction by overcoming the elastic energy of adjacent LC directors. This orientational motion of CNTs produced the local distortion of adjacent LC directors and thus the light leakage to form the vertical stripes. This orientational motion together with transient translational motion under DC field leads us to conclude that our CNTs possess net charges and permanent dipole moment. The net charges of CNTs could be accumulated by the charge transfer from the adjacent interacting LC molecules or by trapping ions that remained usually in the LC cell.[25] Some thick stripes were also visible through optical microscope, although most vertical stripes did not leave their physical traces under optical microscope. They were seemingly connected between two electrodes at above 60 V with 60 Hz but their persistent motion between two electrodes at low frequency response was clearly visible, which will be discussed in the next paragraph.

Understandings of the pattern formation from two different cells can be described in terms of pattern dynamics at low frequency limit of 1 Hz. Although two experiments were done independently, the dynamic response of CNTs from vertical cell and in-plane cell are strongly correlated to each other and are interpreted as the top and side views. When the CNT starts to move normally to the substrate under strong AC bias, the LC molecules nearby will follow the CNT motion (translational and orientational) and generate the tilt angle from the homeotropic alignment of LC directors, giving rise to light leakage. The crossed dark state results from the coincidence of the LC directors with the axes of crossed polarizers. The light leakage with an oriental fan shape (Fig. 4(b)) originates from some phase retardation due to relatively less distorted LC

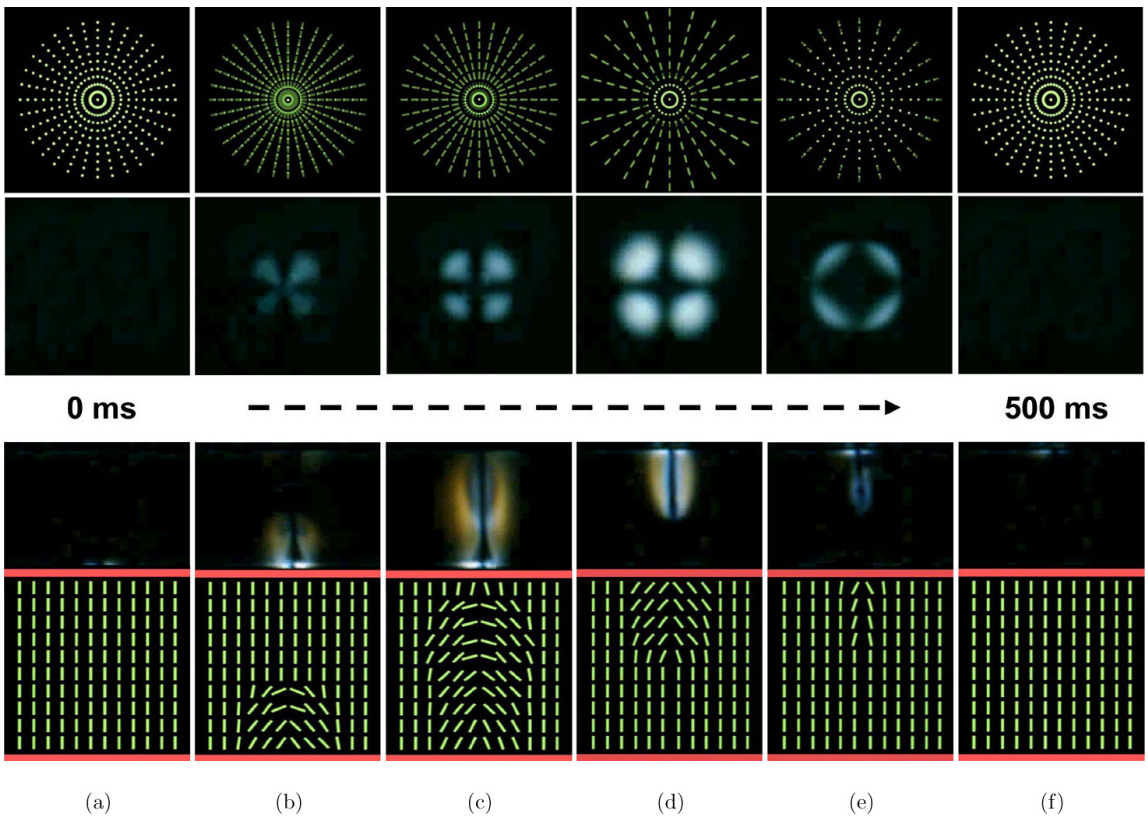

Fig. 4. Two upper panels indicated the schematic and real orientational patterns of the LC directors in the homeotropic vertical cell at 100 V and 1 Hz, and two lower panels are those from the homogeneous in-plane cell at 60 V and 1 Hz. The LC directors in the schematics showed the corresponding dynamic motion of the CNT with time evolution [(a)–(f)]. The LC director appears to be a dot and a bar if one looks at the short and long axes of the LC molecules in a schematic drawing, respectively, i.e., the longer bar indicates the LC director to be tilted down more from vertical alignment in the top panel.

directors from homeotropic alignment.[f] This distortion becomes severe over time (Fig. 4(c)), increasing the light leakage but the dark state at the center becomes wider.

The corresponding pattern changes are also visualized in the in-plane cell (lower panel) which can be regarded as a side view of the vertical cell.

One can clearly see the time evolution of the CNT motion from the bottom to the top and the related LC directors. We see a wider dark state at the center in Fig. 4(c) due to the fact that the LC directors start again to align with the electric field after CNT motion. The increase in the area for light leakage reveals that more LC molecules are deformed in three dimensions by the increased motion of the CNT. When the CNT reaches the other edge of the electrode as can be seen from the bottom panel of Figs. 4(d) to 4(f), most LC directors return back to align perpendicular to the substrate in the homeotropic cell after the CNT motion. These motions are reproduced repeatedly over time.[g]

The spot distribution can present useful information on how well CNTs are dispersed in LC medium, which is not easily accessible in conventional approaches.

The number of spots are field-strength dependent. This can be explained by the incremented velocity of LC molecule in large field, $a = Eq/m$, where a and E are the acceleration and electric field,

[f]The transmittance is defined by $\sin2(2\psi(V))\sin2(\pi d\Delta n_{\text{eff}}/\lambda)$, where ψ is a voltage-dependent angle between the LC director and crossed polarizer axes, and $d\Delta n_{\text{eff}}$ is also a voltage-dependent effective cell retardation value where d and Δn_{eff} are the cell gap and the effective refractive index, respectively. The motion of CNTs gives rise to the change in effective cell retardation value and thus the transmittance is to be altered.

[g]Additional information is available via http://nanotube.skku.ac.kr/support.html.

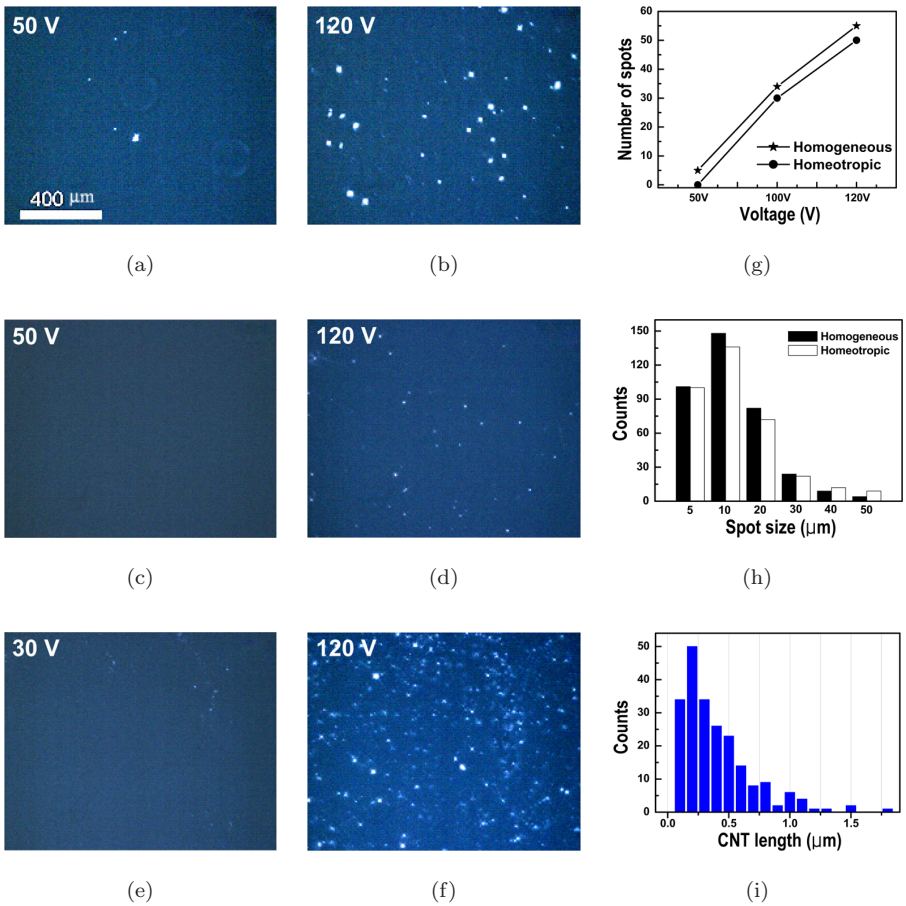

Fig. 5. Polarizing optical micrographs of [(a) and (b)] homogeneous cell and [(c) and (d)] homeotropic cell at a t-MWCNT concentration of 0.001 wt% in terms of AC bias voltage indicated in rms value. Those of SWCNTs at a lower CNT concentration of 0.0005 wt% [(e) to (f)] were provided for comparison. (g) The number of white spots for the corresponding cells at a t-MWCNT concentration of 0.001 wt% as a function of AC bias voltage. (h) The size distribution of white spots which was obtained from 370 data in an area of $2700 \times 2200\,\mu m^2$ at AC bias voltage of 120 V. The resolution was limited to $5\,\mu m$ to cover the large areas. (i) The length distribution of CNTs. The data of 163 CNTs were obtained from AFM images with an area of $4 \times 4\,\mu m^2$ in a contact mode. The scale bar in (a) was applied to all other figures.

respectively, and q and m are the excess charge and mass of CNT, respectively, that leads to the deformation of LC director in far distance. As a consequence, we expect to generate higher spot density and larger spot sizes at higher AC field.

In Fig. 5, we observed that the spot density increased almost linearly with the field strength, although the number of spots and size distributions varied with the CNT densities and initial LC alignments. In case of SWCNT at the same CNT concentration as that of t-MWCNT, the higher spot density was observed due to the presence of more abundant light SWCNTs. The voltage in which spots appeared was also lower than those of other two cells, due to the lighter weight of SWCNTs than t-MWCNTs (Fig. 5(f)). The spot-size distribution for t-MWCNTs is of Gaussian shape being cutoff at low limit and has a maximum peak at $10\,\mu m$ consistently for both homogeneous and homeotropic cells. The sizes smaller than $1\,\mu m$ cannot be visible through optical microscope due to their resolution limit (Fig. 5(h)). The size distribution of CNTs was similar to that of spots, although the mean spot size is bigger than that of CNTs. A more intriguing fact is the spot distribution in Figs. 5(a) to 5(f) that represents the degree of CNT dispersion in LC medium. Thus the pattern dynamics provides useful information for visualizing the degree of dispersion and length distribution of CNTs in LC medium.

4. Conclusion

In summary, we have observed various patterns generated under strong AC field in CNT-doped LC

cells. The density functional calculations presented that LC molecules strongly anchored with a binding energy of $\sim -2\,\text{eV}$ on the CNT wall, which was associated with the formation of helical wrapping to enhance hexagon–hexagon π-overlapping and charge transfer from LC molecule to CNT. The detailed dynamics of patterns proved that these patterns generated under DC/AC field were explained by the presence of excess charges (inducing transient translational motion under DC field) and the permanent dipole moment in rod-like CNTs (inducing orientational motion under strong AC field). We also suggest that the spot counting and their distribution are closely related to the degree of dispersion of the CNTs in the host matrix. The various pattern dynamics of CNTs could be utilized as a molecular rotor in liquids and a light modulator by birefringence induction in the future.

Acknowledgments

This work was supported by grant No. R01-2004-000-10014-0 from the Basic Research program of the KOSEF (SHL) and by the KRF Grant funded by the Korean Government (MOEHRD) (KRF-2005-201-C00012) and in part by the KOSEF through CNNC at SKKU (YHL).

References

1. B. Vigolo, A. Penicaud, C. Coulon, C. Sauder, R. Pailler, C. Journet and P. Bernier, *Science* **290**, 1331 (2000); J. Zhu, J. D. Kim, H. Peng, J. L. Margrave, V. N. Khabashesku and E. V. Barrera, *Nano Lett.* **3**, 1107 (2003).
2. B. J. Landi, R. P. Raffaelle, M. J. Heben, J. L. Alleman, W. VanDerveer and T. Gennett, *Nano Lett.* **2**, 1329 (2002).
3. X. Gong, J. Liu, S. Baskaran, R. D. Voise and J. S. Young, *Chem. Mater.* **12**, 1049 (2000); G. Viswanathan, N. Chakrapani, H. Yang, B. Wei, H. Chung, K. Cho, C. Y. Ryu and P. M. Ajayan, *J. Amer. Chem. Soc.* **125**, 9258 (2003).
4. K. E. Wise, C. Park, E. J. Siochi and J. S. Harrison, *Chem. Phys. Lett.* **391**, 207 (2004); L. Valentini, I. Armentano, J. Biagiotti, A. Marigo, S. Santucci and J. M. Kenny, *Diamond Relat. Mater.* **13**, 250 (2004).
5. D. L. Fan, F. Q. Zhu, R. C. Cammarata and C. L. Chien, *Appl. Phys. Lett.* **85**, 4175 (2004).
6. H. Duran, B. Gazdecki, A. Yamashita and T. Kyu, *Liq. Cryst.* **32**, 815 (2005).
7. M. J. O'Connell, S. M. Bachilo, C. B. Huffman, V. C. Moore, M. S. Strano, E. H. Haroz, K. L. Rialon, P. J. Boul, W. H. Noon, C. Kittrell, J. Ma, R. H. Hauge, R. B. Weisman and R. E. Smalley, *Science* **297**, 593 (2002).
8. R. Bandyopadhyaya, E. N. Roth, O. Regev and R. Y. Rozen, *Nano Lett.* **2**, 25 (2002); R. A. Mrozek, B. S. Kim, V. C. Holmberg and T. A. Taton, *Nano Lett.* **3**, 1665 (2003).
9. M. Zheng, A. Jagota, E. D. Semke, B. A. Diner, R. S. Mclean, S. R. Lustig, R. E. Richardson and N. G. Tassi, *Nature Materials* **2**, 338 (2003).
10. J. Y. Lee, J. S. Kim, K. H. An, K. Lee, D. Y. Kim, D. J. Bae and Y. H. Lee, *J. Nanosci. Nanotech.* **5**, 1045 (2005).
11. M. D. Lynch and D. L. Patrick, *Nano Lett.* **2**, 1197 (2002).
12. M. F. Islam, A. M. Alsayed, Z. Dogic, J. Zhang, T. C. Lubensky and A. G. Yodh, *Phys. Rev. Lett.* **92**, 088303 (2004).
13. I. Dierking, G. Scalia, P. Morales and D. LeClere, *Adv. Mater.* **16**, 865 (2004); I. Dierking, G. Scalia and P. Morales, *J. Appl. Phys.* **97**, 044309 (2005).
14. W. Lee, C.-Y. Wang and Y.-C. Shih, *Appl. Phys. Lett.* **85**, 513 (2004).
15. I. S. Baik, S. Y. Jeon, K. A. Park, S. H. Jeong, K. H. An, S. H. Lee and Y. H. Lee, *Appl. Phys. Lett.* **87**, 263110 (2005).
16. W. Lee and Y.-C. Shih, *J. Soc. Inf. Dip.* **13**, 743 (2005).
17. H. J. Jeong, K. K. Kim, S. Y. Jeong, M. H. Park, C. W. Yang and Y. H. Lee, *J. Phys. Chem. B* **108**, 17695 (2004).
18. K. K. Kim, D. J. Bae, C.-M. Yang, K. H. An, J. Y. Lee and Y. H. Lee, *J. Nanosci. Nanotech.* **5**, 1055 (2005).
19. B. J. Delley, *Chem. Phys.* **92**, 508 (1990); B. Delley, *J. Phys. Chem.* **100**, 6107 (1996).
20. J. P. Perdew and Y. Wang, *Phys. Rev. B* **45**, 13244 (1992).
21. A. D. Becke, *J. Chem. Phys.* **88**, 2547 (1988).
22. S. Yasuyuki, M. Kazutoshi and D. Dietrich, *Liq. Cryst.* **30**, 1371 (2003).
23. K. A. Park, S. M. Lee, S. H. Lee and Y. H. Lee, *J. Phys. Chem. C* **111**, 1620 (2007).
24. S. Elston and R. Sambles, *The Optics of Thermotropic Liquid Crystals* (Taylor & Francis Ltd., London, UK, 1998), p. 250.
25. M. Bremer, S. Naemura and K. Tarumi, *Jpn. J. Appl. Phys.* **37**, L88 (1998).